Effects of Weak Bands on Pillar Stability in Stone Mines: Field Observations and Numerical Model Assessment

Gabriel S. Esterhuizen, Senior Research Engineer
John L. Ellenberger, Lead Research Scientist
NIOSH-Pittsburgh Research Laboratory
Pittsburgh, PA, USA

ABSTRACT

Observations of pillar conditions in limestone mines showed that the presence of weak bands in the limestone can result in pillar damage at stresses that are lower than one would otherwise expect. The objective of this National Institute for Occupational Safety and Health study was to investigate the mechanism of failure caused by the presence of weak bands by using a series of numerical models based on realistic physical properties. The effect of the weak bands on pillar strength was also investigated by developing a series of pillar models with different width-to-height ratios and determining their strength by simulating a servo-controlled loading condition. The material properties of the bands and the limestone were varied and their effects on pillar strength were determined.

Model results demonstrated failure development similar to the pillars observed in the field. The weak bands were seen to develop tensile stresses in the limestone as they extrude under increasing stress. The limestone fails in tension at a much lower stress than its expected uniaxial compressive strength. The results showed the load bearing capacity of the pillars can be reduced significantly by the presence of multiple thin weak bands. The degree of strength reduction is largely dependent on the compressive strength, the frictional resistance and the thickness of the weak bands. Single weak bands do not affect pillars as severely as multiple bands. However, the model results show that a single thick weak band, which comprises more than about 2 percent of the pillar height, can cause a significant reduction in pillar strength. The weakening effect of the bands become less severe as the pillar width-to-height ratio is increased.

Field observation of spalling and failure associated with weak bands in limestone pillars show that the failure mechanism in the models resembles the observed failure. The model results provide insight into the important factors affecting pillar strength in the presence of weak banded materials.

INTRODUCTION

The National Institute for Occupational Safety and Health (NIOSH) has collected data at 34 underground stone mines in a study of factors that influence pillar and roof span stability. During field data collection, it was unusual to see significant pillar damage but in several instances damage was associated with thin weak bands in the pillars (Esterhuizen et al., 2006). These observations prompted an effort to understand the mechanism that produces damage near and between the weak bands and its effect on pillar strength.

Field observations of pillar damage have been discussed in earlier works where pillars exhibited damage in excess of what one would intuitively expect from normal loading (Alber and Heiland, 2001a, 2001b). It has been recognized that rock failure can be the result of purely tensile damage under low confinement. In some cases, tensile crack damage dominated over shear cracks by more than 50 to 1 (Diederichs, 2002). Studies in granite recognized that when confinement is low, extension fracturing is the dominant mode of failure. (Hajiabdolmajid et al., 2002). It has also been concluded that the absence of confinement in slender pillars can result in a brittle failure mode, while wider pillars also combine shearing (Esterhuizen, 2006). In this paper the term "brittle failure" will be used to describe the failure mode of extension fracturing parallel to the major principle stress, as opposed to shear failure where conjugate shear planes develop oblique to the direction of the major principal stress.

The effect of end constraints on the strength of rock samples tested in the laboratory has received much attention in the literature, Jaeger and Cook (1979) give a good overview of the subject. A theoretical analysis of stresses within cylindrical specimens (Peng, 1971) showed that significant tension can be induced if soft extruding end pieces are used in compression testing. Experimental results showed that the strength of granite samples can reduce from as high as 207 to 96 MPa (30,000 to 14,000 psi) by using various end materials in compression testing.

The models described in this paper were constructed and run using the FLAC-2D (Cundall et al., 2005) finite difference program. In addition to the design of a series of basic models with a range of different width-to-height (W/H) ratios, physical properties of the limestone and the weak bands that could contribute to the pillar behavior were addressed. This study utilized the results of laboratory strength tests and the RocLab software to produce realistic properties for the models (Hoek et al., 2002). The effects of parametric variation are also presented and discussed.

FIELD OBSERVATION

During the course of visits to 34 limestone mines in the Eastern and Midwestern U.S. a number of pillars were observed exhibiting varying degrees of failure in association with one or more thin bands of weak material. The failure can manifest itself as a ledge or overhang either above or below a thin bed of material that was notably weaker than the encasing strata, shown in figure 1. The development of overhangs, ledges, and concave zones associated with thin planes of softer material was observed frequently, with the pillar presenting the appearance of being much more heavily loaded than one would expect as a result of simple tributary area pillar loading.

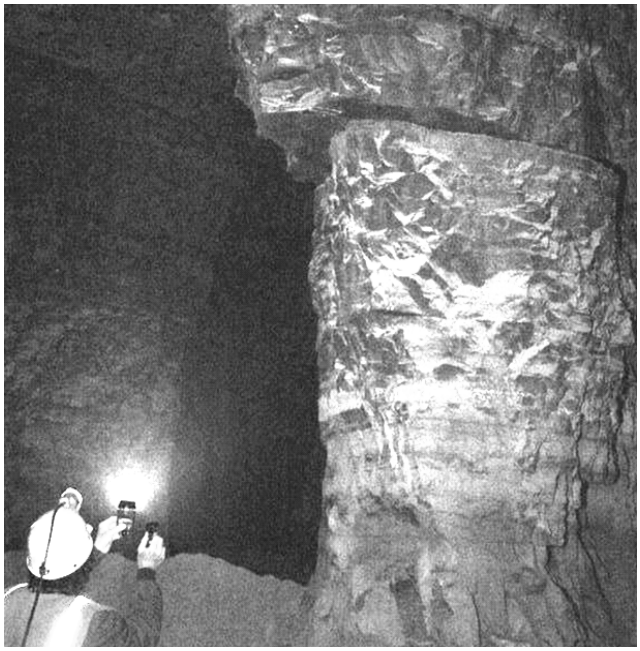

Figure 1. Overhang caused by a weak band in a limestone pillar.

A second failure mode that seemed to occur at higher pillar stress was vertical fracturing and spalling of thin slabs of limestone between the weak bands, shown in figure 2. In this case, the average pillar stress ranged between approximately 15 and 20 MPa (2,700 to 2,900 psi), which was only about 10-15 percent of the uniaxial compressive strength of the limestone beds at this mine.

The material comprising the weak bands observed in the field included carbonaceous bedding planes, calcite fillings on bedding planes, and indurated clays or seat earths that had characteristics more closely resembling soils than rocks. Figure 3 shows an example of a weak band infilling that was easily penetrated by a geologist's pick.

The field observation of pillars showing failure controlled by discontinuities, more specifically bedding, at relatively shallow depths has been documented in other cases (Hoek et al., 1995).

FAILURE MECHANISM

Based on the field observations, it appeared that extrusion of the weak bands contributed to the failure of the stronger limestone. At lower loads, the soft material would extrude and release blocks of limestone defined by pre-existing joints. This causes the overhangs observed in figure 1. At higher vertical loads, the intact limestone

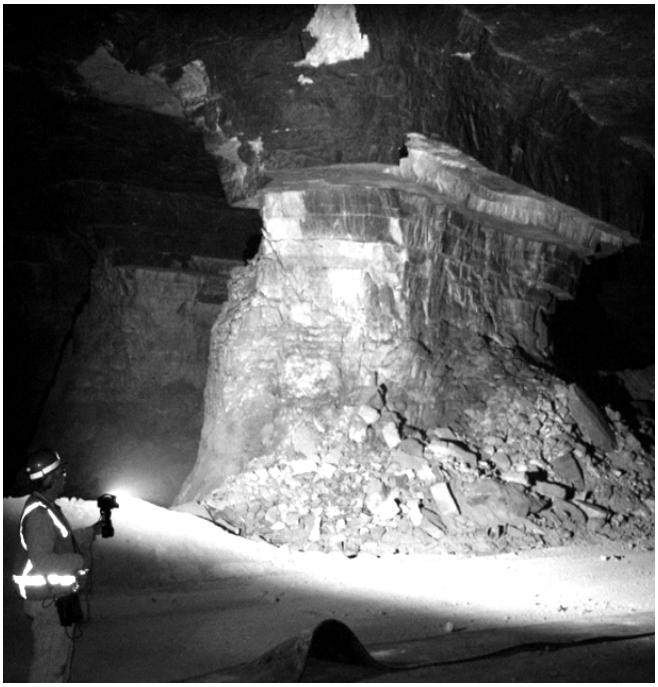

Figure 2. Pillar damage observed in rock containing thin weak bands. Note spalling of the intact rock material between the weak bands.

Figure 3. Low strength weak band showing geologists pick embedded in material.

appears to fracture into thin vertical slabs. It was speculated that this failure is related to horizontal tensile stresses that develop as the weaker material extrudes under the elevated loads. Numerical models were developed to investigate the postulated mechanism of failure.

Model Design

The model to investigate the failure mechanisms simulated a single strong rock slab encased between two weak bands, shown in figure 4, representing a portion of a bedded rock mass. The

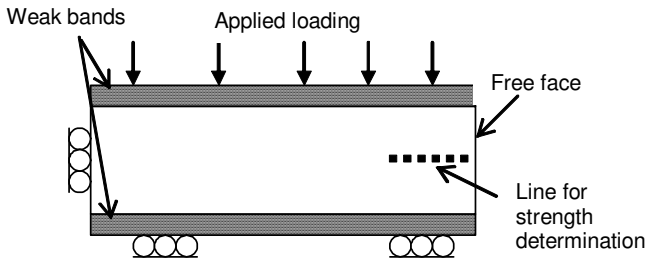

Figure 4. Model layout to investigate failure mechanisms in strong rock encased between two weak bands.

thickness of the weak bands was initially set to 10 percent of the strong rock thickness. The upper and lower boundaries of the model were constrained in the vertical direction. A symmetry plane was defined at the left boundary while the right boundary was a free surface representing an excavation surface, i.e. a pillar rib in this case.

After constructing the models, the physical properties for the limestone and the weak bands were developed. The limestone represented a rock mass with uniaxial compressive strength of 100 MPa (14,000 psi) and Geologic Strength Index (Hoek et al., 2002) of 80. The Roclab software (Hoek et al., 2002) was used to develop the equivalent Coulomb parameters selected for FLAC modeling. The resulting limestone cohesion was 8.83 MPa (1,280 psi) with a friction angle of 38 degrees and tensile strength of 1.0 MPa (145 psi) . The weak band properties were selected from the database of properties in FLAC, and were generally representative of a strong, clayey soil. The initial strength parameters assigned to the weak bands were cohesion of 6.0 kPa (0.87 psi) with a friction angle of 24 degrees. The elastic modulus of the weak bands was initially set to 5% of the strong bed modulus.

It has been recognized that continuum models with traditional failure criteria (e.g. Hoek-Brown or Mohr-Coulomb) based on simultaneous mobilization of cohesive and frictional strength components have not been successful in predicting the extent and depth of brittle failure, often seen as rock-slabbing parallel to the major principal stress. A bilinear failure criterion was therefore used to simulate brittle failure of the rock at low confinement, after Kaiser et al. (2000). At low confinement, the compressive strength of the rock material was set at one third uniaxial compressive strength, but with a zero friction angle to simulate the delayed mobilization of friction associated with brittle failure. When the confining stress exceeds 5 percent of the maximum stress, the friction and cohesion values revert to those developed from the Hoek-Brown failure criterion. Details of the procedure followed are presented in Esterhuizen (2006).

The model was loaded by gradually moving the upper boundary downwards while the lower boundary remained fixed. The response of the model in the vicinity of the free face was monitored by observing stress and failure development as the loading increased. The strength of the rock was determined by averaging the vertical stress at mid-height of the slab near the free face, shown in Figure 4. Being near the free face, the average stress in this region approximates the uniaxial compressive strength of the rock mass consisting of the combined weak bands and strong rock. The reason for modeling a wide slab of rock, rather than say a cube, was to observe how failure propagates from the free face towards the interior of the slab.

Model Results

The effect of the weak bands on the strength of the slab model was assessed by determining the strength of the slab for various scenarios. A uniform rock slab model, consisting of only the stronger rock material, had a strength of 35 MPa (5,000 psi), which is approximately equal to the brittle strength of the material. When weak bands are added, the strength is reduced by 80 percent to 6.8 MPa (1,000 psi).

Inspection of the model output showed that failure of the layered rock mass occurs through an extrusion-tension mechanism. As the vertical load is increased, failure first occurs in the weak bands, because they are essentially cohesionless. As the load continues to increase, a zone of tension develops within the stronger slab (figure 5a), which is caused by the extrusion of the failed weak bed material. As the loading increases, the tensile stresses increase and tensile failure develops in the stronger slab (figure 5b), which relieves the initial zone of tension (Figure 5c). As the vertical loading continues to increase, tensile stresses are induced on either side of the initial tensile failure zone and tensile failure continues to occur. The process repeats until the entire slab has failed or the extrusion mechanism is inhibited by frictional resistance between the weak bands and the rock slab. If the tensile failure process is inhibited, the remainder of the slab fails by Coulomb shearing. The extrusion-tensile failure mechanism can explain the observed progressive spalling of intact rock at relatively low stress, shown in figure 2.

The sensitivity of the rock mass to parameters such as elastic modulus of the weak bands, the strength of the weak bands and the tensile strength of the stronger material was tested. Variation of these parameters showed that the extrusion-tensile failure mode occurred for most scenarios. However, as the weak bands become stronger and stiffer, the role of tensile failure is diminished and Coulomb shear failure of the strong rock slab becomes more prevalent. On the contrary, when weak bands are thick and weak, extrusion without tensile failure tends to occur.

PILLAR MODELING

The simple slab model described above does not resemble a mine pillar, and the effect of weak bands is expected to be different when they occur within a mine pillar. Failure development in a mine pillar is affected by the end constraints provided by the roof and floor contacts, the pillar shape and by the initial stress state. Therefore, a series of models were developed to evaluate the effect of weak bands on typical pillars found in limestone mines.

Model Design

A series of models were developed to simulate a pillar and the surrounding roof and floor rocks. The models were designed so the roof, pillar, floor and weak bands can be independently assigned physical properties. The weak bands were evenly distributed vertically throughout the pillar. The roof and floor contacts were also assigned as weak bands. Initially the thickness of the weak bands was 3 percent of the thickness of the limestone beds. The models ranged in width-to-height ratio from 0.3 to 1.5 to bracket the typical range of width-to-height ratios observed in the field. The range of width-to-height ratios modeled was achieved by maintaining a constant model pillar width while changing the height. The weak bands were generated with three rows of elements each in order to permit distortion of the weak material.

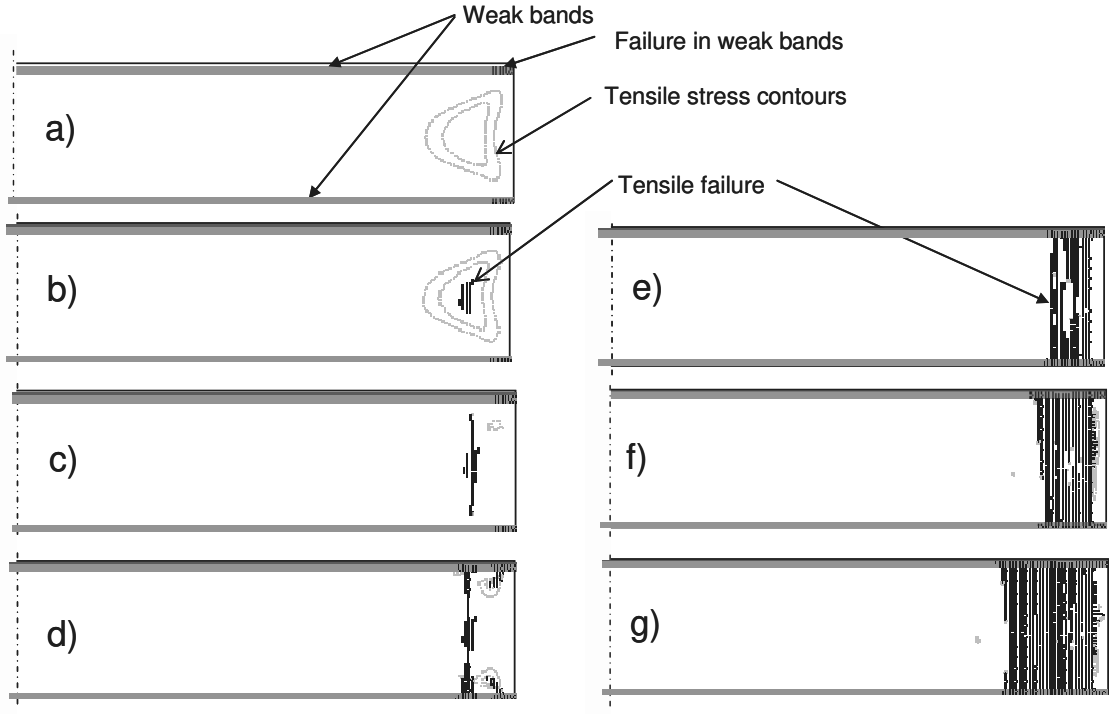

Figure 5. Stages of failure development in a beam of strong rock encased between two weak bands.

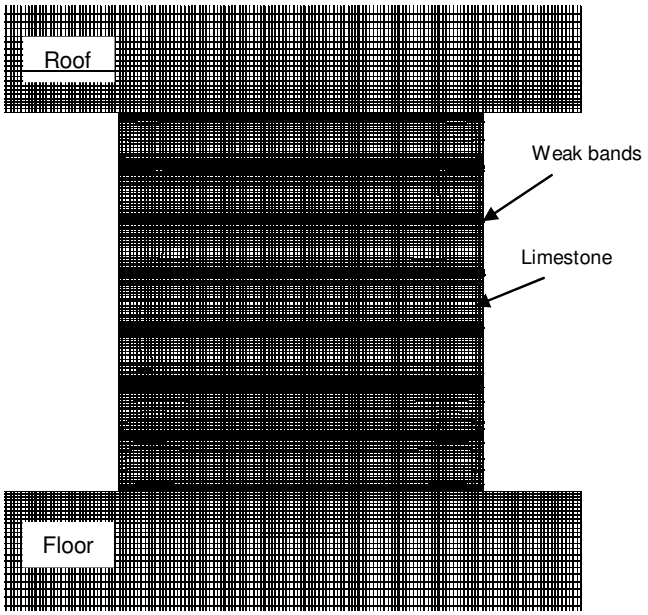

Figure 6. Part of a pillar model showing level of detail and variation of element sizes to accommodate thin weak bands. Pillar width-to-height ratio is 1.0.

Figure 6 shows the element discretization used in a pillar with width-to-height of 1.0.

The initial strength parameters were the same as described above for the simple slab models. The strength properties of the weak bands and the limestone were varied to investigate their effect on pillar strength. The thickness of the weak bands and number of bands was also varied.

The pillar model was loaded by slowly moving the upper boundary of the model downwards, using the servo-control function available in FLAC. The function controls the velocity of the upper boundary by considering the unbalanced forces in the model. If failure occurs the rate of loading is slowed or stopped until the excessive loads have been dissipated, after which the velocity is increased again to continue loading the model. The average stress at mid height of the pillars was computed and recorded during the loading process. The pillar strength was defined as the peak value of the recorded average stress. The models were loaded until the recorded average stress had dropped 20 percent below the peak value.

Validation of Un iform Pillar Models

Validation of the model results was carried out by comparing the model-predicted pillar strength for pillars without weak bands to the pillar strength equation proposed by Obert and Duvall (1967):

$$S = \sigma_p(0.778 + 0.222\frac{w}{h})$$

where σ_p is the strength of a pillar with a width-to-height ratio of 1.0, w is the pillar width and h is the pillar height. Model results for a uniform rock mass, without any weak bands, are shown against the equation in Figure 7. The value of σ_p in the equation was set to 26.4 MPa (3,800 psi), so that it would be normalized to the numerical model results. It can be seen that the model predicted strength follows a similar trend as that predicted by the equation. It was concluded that the modeling method provides a realistic representation of pillar strength over the range of width-to-height ratios shown. The strength and elastic parameters of the limestone were kept unchanged in all the model runs, except when sensitivity to the limestone tensile strength was investigated.

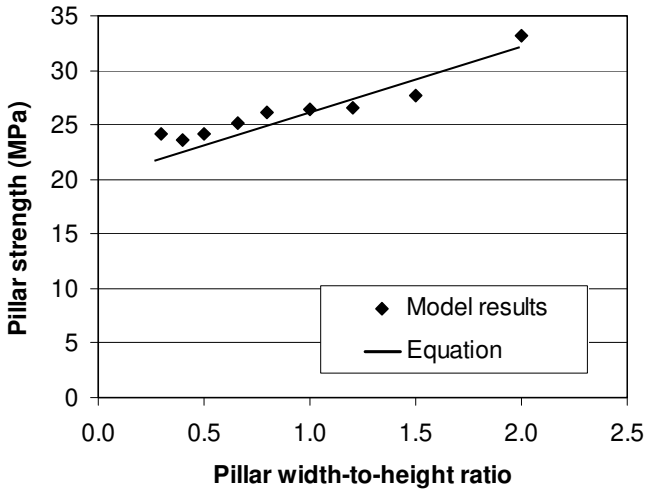

Figure 7. Graph showing modeled pillar strength for a uniform rock mass compared to the Obert-Duval (1967) equation for pillar strength.

PILLAR MODELING RESULTS

The Effect of Adding Weak Bands

Weak bands with cohesion of 6 kPa (0.87 psi) and friction angle of 24 degrees were added to the models using the initial strength parameters and were loaded until the peak pillar strength was exceeded. The presence of the weak bands considerably reduced the pillar strength. An examination of the development of failure in the models showed that a uniform rock mass initially fails in a brittle-compressive mode and shear failure occurs through the pillar core during the final stages of failure (figure 8a and 8c). Failure in the weak-banded models initiated as tensile splitting at the outer extremities of the pillars, similar to the mechanism observed in the field and identified in the slab models (figure 8b). As the load increased, the tensile splitting would continue and, in the case of slender pillars, can extend right through the pillar. In the wider pillars, the tensile splitting process is inhibited by the frictional resistance provided by the roof and floor rocks. In these cases, the pillar loses some of its effective width to the tensile-extrusion failure mode, and ultimately fails by shearing of the pillar core shown in figure 8d.

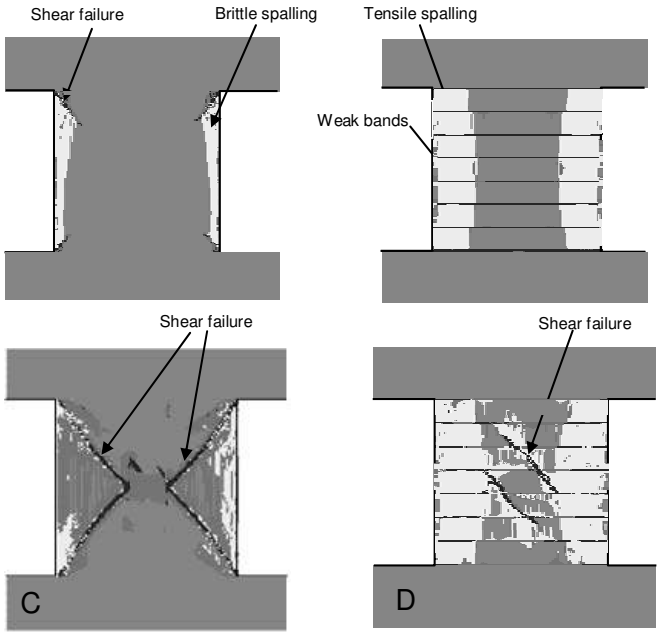

Figure 8. Model results showing rock failure in pillars without and with weak bands. Pillar (a) consists of uniform rock and (b) contains weak bands. Both are loaded to 80 percent of their peak strength. Pillars (c and d) are uniform and banded respectively, and both have been loaded beyond their peak strength.

Figure 9 shows the change in pillar strength for width-to-height ratios of 0.3 to 1.5 due to the presence of thin and thick weak bands in the models. The thin and thick weak bands were 7% and 13% of the limestone bed thickness, respectively. It can be seen that the reduction in pillar strength is affected by the pillar width-to-height ratio and the weak bed thickness. For example, the models with a 0.5 width-to-height ratio and thin weak bands showed a drop in peak strength to about 25 percent of the uniform pillar strength. Significantly, the pillars with width-to-height ratios of greater than 0.8 did not show such a large drop in strength. A greater thickness of the weak bands results can result in a very significant loss of pillar strength.

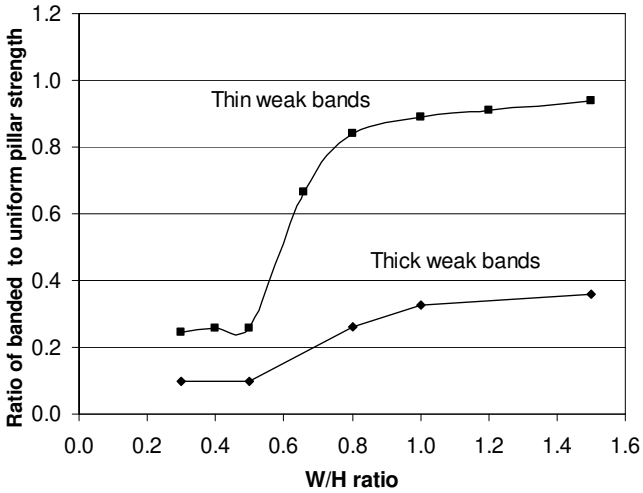

Figure 9. Model results showing strength reduction caused by the presence of multiple weak bands in pillars. Thin weak bands are 3% and thick weak bands 7% of the limestone bed thickness respectively. Friction angle is 24 degrees with 6 kPa (0.87 psi) cohesion.

It appears, therefore, that the strength of slender pillars containing weak bands can be significantly reduced by the extrusion-tensile failure mode. However, wider pillars are compromised to a lesser extent.

The Effect of Weak Band Strength

The initial pillar models all had weak bands with strength equivalent to that of a weak clayey soil, which had a compressive strength of only 0.1% of the strength of the limestone beds. A series of additional models were run to determine how the pillar strength would be affected by bands that were not as weak. The strength of the weak bands was increased in stages up to 38 percent of the strength of the limestone that comprised the remainder of the pillar.

The results for the pillars containing thin weak bands are presented in figure 10. The results show that the effect of the weak bands on pillar strength is again dependent to the width-to-height ratio of the pillars. When the weak bands are relatively strong, they have little effect on the wider pillars, in some cases the models showed an increase in strength when the bands are strong, this is thought to be a secondary effect of the loading rate and interaction between extrusion and compressive failure which produces variable model behavior. The weak bands reduce the strength of the more slender pillars to a greater extent than the wider pillars.

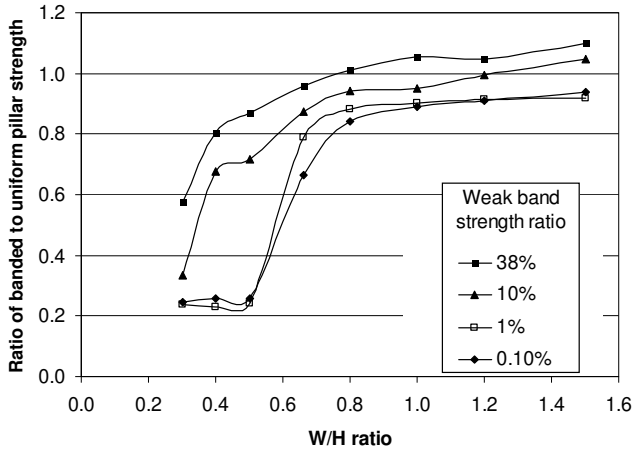

Figure 10. Model results showing the effect of the strength of multiple weak bands on pillar strength. Weak band strength is expressed as a percentage of the limestone strength. Weak band thickness was 3% of the limestone bed thickness, with 24 degrees friction angle and 6 kPa (0.87 psi) cohesion.

The Effect of Weak Band Friction

The sensitivity of the pillar strength to weak-band friction was tested by conducting a further set of runs using the model with thin weak bands. For these analyses the weak-band friction was varied from 18 to 35 degrees. The resulting pillar strengths are presented in figure 11. The results show that as the weak-bed friction decreases, the pillar strength is decreased. Similar to the previous results, slender pillars experience a greater decrease in strength compared to the wider pillars. However, low friction values, such as 18 degrees, can also result in large reductions in the strength of the wider pillars.

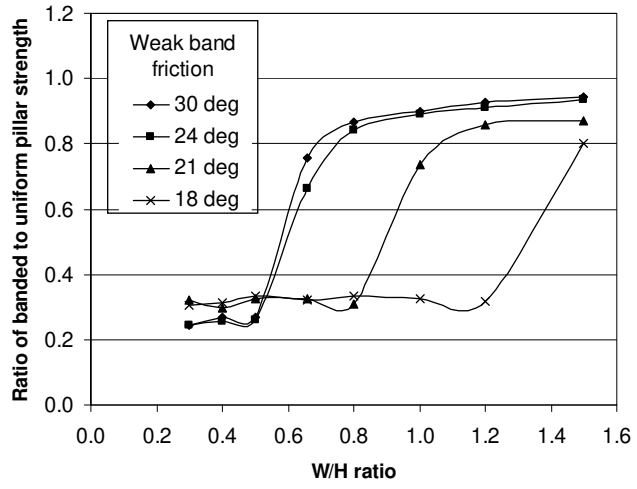

Figure 11. Model results showing the effect of the friction angle of multiple weak bands on pillar strength. Weak band thickness was 3% of the limestone bed thickness. Weak band cohesion was 6 kPa (0.87 psi) in all the runs.

In practical situations, the presence of moisture can further reduce the friction between the weak bands and the surrounding rock, either by lubricating the contact planes or by an increase in the pore-pressure within the weak bands as pillar load is increased. In such cases, the frictional resistance can be reduced to almost zero and pillar strength is likely to be further reduced.

Effect of Limestone Tensile Strength

The relationship between pillar strength and tensile strength of the limestone was also evaluated. The base case material properties included a tensile strength of the limestone of 1 MPa (145 psi). The influence of a lower tensile strength of 0.5 MPa (72 psi) was tested on both uniform pillars and pillars containing thin weak bands. A lower tensile strength resulted in little change in the peak strength of the uniform pillars regardless of the width-to-height ratio. This result is expected, since tensile failure does not play a role in the failure of uniform pillars. However, the pillars with width-to-height ratios of 0.5 or less, that contain weak bands, showed strength reduction of about one half the strength shown in figure 9. Wider pillars did not show a material reduction in strength.

Effect of Elastic Modulus Ratio

Models were also modified to establish the impact of various elastic moduli of the weak bands. It was argued that the elastic extrusion of the weak bands should have an effect on the induced tension in the stronger limestone, and therefore reduce the pillar strength. The elastic modulus of the weak bands was varied from 0.1 through 10 percent of the limestone modulus using a 1.0 width-to-height model with weak bands having a 24 degree friction angle. It was determined that only when the weak band modulus dropped below 1.0 percent of the limestone modulus did it have a significant effect on the pillar strength.

Single Weak Bands

The analyses reported so far were all conducted with multiple weak bands in the pillars. Models of pillars containing single weak bands showed that the strength is not affected as severely as when multiple weak bands are present. Figure 12 shows how the presence of a single weak band at mid-height of a pillar can affect the strength of a pillar with width-to-height of 1.0. In these models the weak bands all had 6 kPa (0.87 psi) cohesion and 24 degree friction angle but the thickness of the weak bed was varied. It can be seen that a single thin weak band has an insignificant effect on the pillar strength, however, as the thickness is increased, its effect on pillar strength becomes significant. When the single weak band was 13 percent of the pillar height, it was found that failure is confined to the weak band only and the stronger limestone does not fail in tension. Under these conditions, the failure mechanism is simply the extrusion of the weak band and the pillar strength is determined by the weak band properties.

During the field studies, pillars were observed that contained single weak bands up to 15 cm (6 in) wide. Most of these pillars did not show any signs of tensile spalling of the intact rock, but joint defined blocks were ejected on occasion. A review of the data

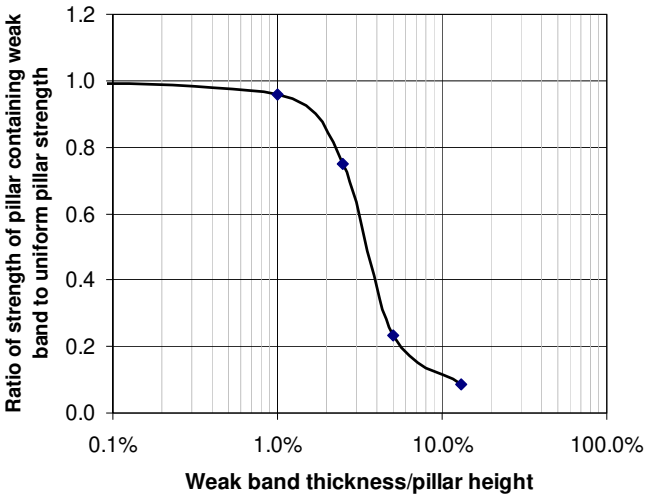

Figure 12. Model results showing the effect of the thickness of a single weak band on the strength of a pillar with width-to-height of 1.0. Weak band friction angle was 24 degrees and cohesion 6 kPa (0.87 psi) in all the runs.

showed that the pillar stresses were in the range of 5 to 11 MPa (700 to 1,600 psi), which did not initiate the extrusion-spalling mechanism.

SUMMARY AND CONCLUSIONS

The model studies have shown that weak bands can significantly reduce the strength of pillars. The observed pillar instabilities associated with weak bands can be explained by a mechanism of extrusion of the weak bands followed by tensile failure of the strong rock layers. The models are a simplification of reality, but are useful for understanding the mechanisms of failure and the sensitivity of pillar strength to the relevant parameters. The study has shown that:

1. The extrusion-tensile failure mode typically initiates at the perimeter of a pillar and progresses inwards, reducing the effective width of the pillar.
2. Observations in operating mines show that weak bands can cause rib failure to initiate when the average pillar stress is only about 10 percent of the limestone strength.
3. Slender pillars (width-to-height<1.0) are more severely affected by the presence of weak bands than wider pillars.
4. Pillar strength is adversely affected as the thickness of the weak bands increase.
5. Model results show that single weak bands can have a significant effect on pillar strength if their thickness exceeds about 2 percent of the pillar height.

The failure mechanism in a pillar with weak bands is predominantly caused by extrusion of the weak bands, which induces tension in the stronger rock slabs. The strong rock fails in tension, which is manifested as rib spalling in underground limestone mines. At lower stresses the extrusion process can release blocks defined by joints or blasting fractures.

The extrusion-tension failure mechanism and model results appear to adequately explain the observed failure of pillars containing weak bands at relatively low stress. The results have helped to develop an understanding of the failure mechanism associated with weak bands in limestone pillars and have shown which parameters are important to consider when designing pillars that may contain weak bands. The information can be used to design safer pillar layouts in limestone mines.

REFERENCES

Alber, M. and Heiland, J. (2001a). Investigation of a Limestone Pillar Failure Part 1: Geology, Laboratory Testing and Numerical Modeling. Rock Mech & Rock Eng *34*(3):167-186.

Alber, M. and Heiland, J. (2001b). Investigation of a Limestone Pillar Failure Part 2: Stress History and Application of Fracture Mechanics Approach. Rock Mech & Rock Eng *34*(3):187-199.

Cundall et al., (2006) Fast Lagrangian Analysis of Continua. Manuals, 6 volumes, Itasca Consulting Group, Minneapolis, Minnesota.

Diederichs, M.S. (2002). Stress Induced Damage Accumulation and Implications for Hrd Rock Engineering. Proceedings of the5th NARMS-TAC Conference, University of Toronto, pp. 889-897.

Esterhuizen, G.S., Iannacchione, A.T., Ellenberger, J.L. and Dolinar, D.R. (2006). Pillar Stability Issues Based on a Survey of Pillar Performance in Underground Limestone Mines. Proceedings of the 25th International Conference on Ground Control in Mining, Morgantown, WV, pp. 354-361.

Esterhuizen, G.S. (2006). An Evaluation of the Strength of Slender Pillars. SME Preprint No. 06-003, 7 p.

Hajiabdolmajid, V., Kaiser, P.K. and Martin C.D. (2002). Modelling Brittle Failure of Rock. International Journal of Rock Mechanics and Mining Sciences, vol. 39, pp. 731-741.

Hoek, E, Carranza-Torres C, and Corkum, B. (2002). Hoek-Brown Failure Criterion – 2002 Edition. Proceedings of the 5th NARMS-TAC Conference, University of Toronto, pp. 267-273.

Hoek E., Kaiser P.K. and Bawden, W.F. (1995). Support of Underground Excavations in Hard Rock. A Balkema, Rotterdam, 215p.

Jaeger J.C. and Cook N.G.W. (1979). Fundamentals of Rock Mechanics, Third Edition, Chapman and Hall, London, 576 p.

Kaiser, P.K., Deiderichs, M.S., Martin, C.D., Sharp J., and Steiner, W. (2000). Underground Works in Hard Rock Tunnelling and Mining. Invited Keynote Address: GeoEng 2000, International Conference of ISRM, Melbourne, vol., 1, pp. 841–926.

Obert, L. and Duvall, W.I. (1967). Rock Mechanics and the Design of Structures in Rock, Wiley, New York, 650 p.

Peng, S.D. (1971). Stresses Within Elastic Circular Cylinders Loaded Uniaxially and Triaxially. Int J of Rock Mech and Min Sci, vol. 8, pp. 399-432.